Constraint on Net Long Term Climate Feedback to Emerge From Satellite Observed Internal Variability by Mid 2040s

Alejandro Uribe[1]*, Frida A.-M. Bender[1], and Thorsten Mauritsen[1]

[1]Stockholm University, Department of Meteorology and Bolin Centre for Climate Research, Stockholm, Sweden

Key Points:

- The strength of forced climate feedbacks is related to its internal variability feedbacks in climate models
- Satellite observations and reanalysis show that models with moderate longwave and shortwave feedbacks are more realistic
- However, constraining net feedback will require longer satellite records, about 60 years in total

*Current address: Department of Meteorology, Stockholm University, 106 91, Stockholm, Sweden.

Corresponding author: Alejandro Uribe, `alejandro.uribe-cortes@misu.su.se`

Abstract

Climate feedbacks are vital in shaping the extent of global warming. While directly observing climate feedbacks is hardly feasible, it is possible to establish a relationship between them and top-of-the-atmosphere flux changes in response to natural fluctuations in surface temperature. In this study, we explore this method to potentially constrain climate feedbacks in climate models using observations. Our findings reveal significant correlations for longwave and shortwave feedbacks within a period of 14 years. This allows for utilizing satellite observations and reanalysis to show that models exhibiting moderate negative longwave and moderate positive shortwave internal variability feedbacks demonstrate better consistency with observations. The emergence of the relationship for the net feedback requires a longer time, about 60 years. Continuous satellite records need to be maintained minimum until the mid-2040s before estimates of observed net internal variability feedback can be used to constrain net forced climate feedback, and thereby climate sensitivity.

Plain Language Summary

Climate feedbacks play a crucial role in determining global warming, but directly observing them is challenging. However, it is possible to establish a connection between these feedbacks and changes in the Earth's energy balance at the top of the atmosphere caused by natural variations in surface temperature, namely internal variability feedbacks. In this study, we investigate this approach to reduce uncertainties in climate feedbacks from the latest generation of climate models, which are widely used for future climate projections. Our results show that relationships between climate feedbacks and internal variability feedbacks exist in these models. We find significant correlations between longwave and shortwave feedbacks over a relatively short period of 14 years. Models with moderate negative longwave and moderate positive shortwave internal variability feedbacks align better with observations. However, establishing a significant relationship for the net feedback requires a longer period of around 60 years. This implies that continuous satellite records need to be maintained at least until the mid-2040s before using observed internal variability feedback to constrain net forced climate feedback and understand climate sensitivity more accurately.

1 Introduction

The increasing levels of atmospheric carbon dioxide have significant implications for the Earth's climate system. Elevated carbon dioxide concentrations enhance the absorption and emission of infrared radiation in the atmosphere, leading to a radiative imbalance at the Top of the Atmosphere (TOA) and subsequent warming of the troposphere (NRC, 1979). The long-term response of global temperatures to this radiative forcing is influenced by a complex interplay of feedback mechanisms, including temperature, water vapor, lapse rate, surface albedo, clouds, and biogeochemical processes. These feedback mechanisms play a crucial role in either amplifying or mitigating the initial warming signal and collectively determine the Equilibrium Climate Sensitivity (ECS), which quantifies the global temperature response to a doubling of atmospheric carbon dioxide concentrations relative to pre-industrial levels.

Generally, in estimating forced climate feedbacks, tools such as theory, observations, climate models, and fine-scale simulations are commonly utilized (Sherwood et al., 2020). Climate models are particularly important as they are designed to solve the complex equations governing the Earth's climate system. However, climate models need to parameterize unresolved processes by establishing empirical relationships with explicitly resolved variables (Williamson et al., 2021). While climate models share fundamental equations, the use of different parameterization approaches among models introduces variations in future projections, including forced climate feedbacks, leading to a range of model-estimated

ECS. Assessing how models represent forced climate feedbacks is challenging due to the absence of long-term global observations spanning decades or centuries. Consequently, reducing uncertainty in model-estimated forced climate feedbacks becomes a complex task. However, if a significant and physically explainable relationship emerges across climate models between observable properties of the climate system and forced climate change, past climate observations can be employed to constrain these feedbacks.

Several studies have identified relationships between various observables and forced climate feedbacks across different generations of models (Forster et al., 2021). For instance, elements of the present mean state have been utilized (e.g., Trenberth & Fasullo, 2010; Brient et al., 2016), as well as past climate change (e.g., Hargreaves et al., 2012; Jiménez-de-la Cuesta & Mauritsen, 2019; Renoult et al., 2020) and internal variability (Dessler, 2013; Mauritsen & Stevens, 2015; Dessler et al., 2018; Dessler & Forster, 2018). Focusing specifically on tropical clouds, Loeb et al. (2018) identified a robust relationship between cloudy-sky flux on timescales of 2.5 to 3 years and ECS. However, they noted that 100 years of data are necessary for this relationship to become statistically robust. Using models from the Coupled Model Intercomparison Project phase 6 (CMIP6), Lutsko et al. (2021) found significant relationships between 50 years of cloud variability and regional forced climate cloud feedbacks across most regions, with the exception of a latitudinal band from 60°N to 90°N. Similarly, Uribe et al. (2022) employed CMIP6 models and demonstrated that the strength of forced climate feedbacks is associated with TOA flux changes in response to natural variations of surface temperature (internal variability feedbacks) from 2001 to 2014. However, they found that this relationship did not hold for net feedback. Additionally, they concluded that uncertainty in simulated and observed internal variability feedbacks over this short period precludes the establishment of an emergent constraint on forced climate feedbacks.

In this study, our primary objective is to contribute to the reduction of uncertainties in forced climate feedbacks by advancing our understanding of the use of observations and the relationships between internal variability feedbacks and forced climate feedbacks in CMIP6 models. Building upon previous research, we specifically investigate the underlying reasons for the lack of a significant relationship between net internal variability and forced climate feedback, despite significant relationships being found for longwave and shortwave feedback components in CMIP6 models. To achieve this, we focus on the period where historical simulations overlap with the available satellite data record. Furthermore, we explore whether the limitations encountered in using observations to constrain forced climate feedbacks persist when utilizing longer historical periods to estimate internal variability.

2 Materials and Methods

We study the relationship between feedbacks arising from internal variability and external forcing in both coupled ocean-atmosphere (CMIP) and atmosphere-only (AMIP) models participating in CMIP6. To accomplish this, we utilize historical simulations and experiments where atmospheric carbon dioxide concentrations are abruptly quadrupled from pre-industrial levels and subsequently held constant (abrupt4xCO2). To capture the range of possible historical climate outcomes and obtain robust estimates of internal variability feedbacks, we utilize up to 5 realizations of historical ensemble members (Table S1). This approach represents an advancement over the study conducted by Uribe et al. (2022), who only employed one ensemble member. By including multiple ensemble members, we can better account for differences in initial states and obtain a more comprehensive estimation of internal variability feedbacks.

In order to quantify feedbacks, we use the planetary energy balance at TOA:

$$R = F + \lambda T \tag{1}$$

where R is the net TOA radiative flux anomaly, F is the radiative forcing, λ is the radiative feedback parameter and T is the surface temperature anomaly (Gregory et al., 2004; Dessler et al., 2018).

We calculate forced climate feedbacks using linear Ordinary Least Squares (OLS) regression coefficients between annual global averages of TOA flux anomalies and T, where the anomalies are calculated as the difference between abrupt4xCO2 and pre-industrial experiments. For the estimation of internal variability feedbacks, we adopt a distinct approach to ensure robust results. We utilize detrended and deseasonalized monthly anomalies derived from various historical ensemble members. However, it is crucial to account for the presence of autocorrelation in the temperature time series within each individual realization. This autocorrelation has the potential to impact the estimation of regression coefficients and standard errors when performing an OLS regression on the combined data. To address this concern, we employ Generalized Least Squares (GLS) instead of OLS. GLS is an extension of OLS that involves transforming the original data into a new set of weighted variables. These weights are determined by computing autocorrelation coefficients through fitting autoregression models of order one, which effectively capture the autocorrelation presence in the data. Subsequently, the transformed data is subjected to OLS regressions to estimate the regression coefficients. Finally, to determine the uncertainty associated with the regression coefficients, we calculate 5-95% confidence intervals using a two-tailed t-test that takes into account the variability in the data and provides confidence intervals that encompass both positive and negative deviations from the estimated regression coefficients.

We conduct a comparison between model results and observed internal variability feedbacks using TOA fluxes from the Clouds and the Earth's Radiant Energy System (CERES) instruments, Energy Balanced and Filled (EBAF) dataset updated to Ed4.1 (Loeb et al., 2018), and gridded temperature anomalies from HadCRUT version 5 (Morice et al., 2021). The comparison is performed during the overlapping period of the CERES-historical simulation (2001-2014). The objective is twofold: to identify models whose internal variability feedback differs from observations, providing valuable insights into their representativeness of forced climate feedbacks, and to investigate the lack of significant relationships between net internal variability and net forced climate feedback despite the presence of significant relationships for the longwave and shortwave components, as reported in previous research (Uribe et al., 2022).

Furthermore, to explore the evolution of the relationship between internal variability and forced climate feedbacks as well as observed and simulated internal variability uncertainties over a longer historical time period (1959 to 2014), we utilize TOA fluxes and sea surface temperatures derived from the ERA5 reanalysis data (Hersbach et al., 2020). Lastly, we assess the necessary conditions for a stable relationship to emerge between net internal variability and net forced climate feedbacks. This information will provide valuable insights into the time scale necessary for robust and reliable assessments of these relationships and will enhance our understanding of the complexities surrounding the relationships between internal variability and forced climate feedbacks.

3 Results

3.1 Internal Variability and Forced Climate Feedbacks Relationship During the CERES Period

In order to be able to use internal variability to constrain long-term feedback there must exist a statistical relationship between these quantities. Indeed, during the overlapping years of CERES satellite observations and historical CMIP6 simulations, there are high correlations between simulated internal variability and forced climate feedbacks (Figures 1a and 1b). Importantly, our results demonstrate a stronger correlation between

internal variability and forced climate feedbacks compared to the findings reported by Uribe et al. (2022). We attribute this improvement in correlation strength to two factors: the inclusion of more models, allowing for a broader range of model representations and variations in internal variability to be captured, and the utilization of additional ensemble members, which enhances the robustness and representativeness of our internal variability feedbacks. These factors combine to provide a more comprehensive representation of the relationship between internal variability and forced climate feedbacks.

To assess the significance of the high correlations over this relatively short period, we conducted a Monte-Carlo test to determine the probability of obtaining correlation coefficients that are equal to or greater than those observed between internal variability and forced climate feedbacks. This analysis involved generating a probability distribution of correlation coefficients by randomly permuting the datasets 100000 times and calculating the correlation coefficients for each permutation. The results (Figure S1) reveal a likelihood of less than 5% that the longwave and shortwave correlation coefficients would occur by chance alone and indicate a strong and meaningful relationship between the strength of longwave and shortwave forced climate feedbacks and their corresponding internal variability feedback. By considering these relationships, observations have the potential to constrain and limit the uncertainties associated with forced climate feedbacks. The comparison between simulated and observed internal variability feedbacks indicates that models exhibiting strong negative and weak negative internal variability longwave feedbacks, as well as models displaying both strong negative and strong positive shortwave internal variability feedbacks, are less consistent with observed data (Figure 2).

In contrast, when combining the longwave and shortwave feedbacks to calculate the net feedback, we do not observe a statistically significant relationship between internal variability and forced climate feedback (Figures 1c and S1). The weak relationship between net internal variability and net forced climate feedback is reflected in the small slope observed in the linear regression (dashed lines in Figure 1c), which indicates a limited association between the two variables. The underlying cause of this weak relationship can be attributed to the relatively larger dispersion or variability in net internal variability feedback compared to that of the net forced climate feedback (variance of 0.27 $W^2\ m^{-4}\ K^{-2}$ compared to 0.14 $W^2\ m^{-4}\ K^{-2}$ for CMIP, and 0.42 $W^2\ m^{-4}\ K^{-2}$ compared to 0.15 $W^2\ m^{-4}\ K^{-2}$ for AMIP). The dispersion of the net internal variability feedback can be largely attributed to the shortwave component, as the variance of the net internal variability feedback is the sum of the variances of the longwave and shortwave internal variability feedbacks (Figure S2). Further examination highlights that cloud radiative effects, in deep convective and stratocumulus regions, primarily influence the dispersion of the shortwave internal variability feedback (compare top, center, and bottom panels in Figure 3). Moreover, it is generally observed that shortwave and longwave feedbacks exhibit a balancing effect, whereby positive shortwave feedback is typically counterbalanced by negative longwave feedback, and vice versa. To quantify the degree of balancing, we calculated the correlation coefficient between longwave and shortwave feedbacks. The analysis indicates that internal variability feedbacks ($r = -0.62$) are less compensated compared to forced climate feedbacks ($r = -0.75$) and suggests that the interplay between shortwave and longwave feedbacks is less effective in offsetting each other within the internal variability context, as opposed to the forced climate feedbacks where the compensation is more pronounced.

Thus, the lack of statistical significance for the net feedback can be attributed to two main factors. Firstly, the large dispersion observed in the shortwave internal variability feedback, particularly in relation to cloud radiative effects in deep convective and subtropical stratocumulus regions. Secondly, the anti-correlation between longwave and shortwave feedbacks, which weakens the overall net signal. These combined factors contribute to the absence of a significant relationship in the net feedback analysis. In the

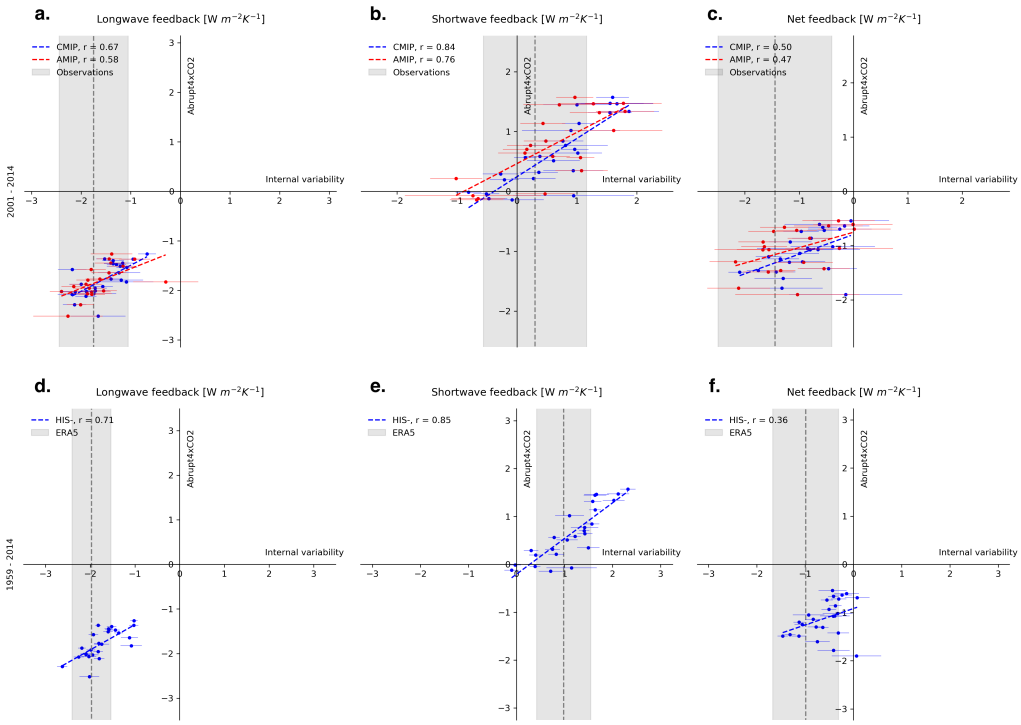

Figure 1. Abruptly quadrupled CO_2 increases versus global internal variability feedbacks and their linear regression (dashed lines) for longwave (left), shortwave (center) and net (right) over CERES (a., b., c.) and ERA5 (d., e., f.) periods. Legends include the correlation coefficient, r, between abrupt and internal variability feedbacks for coupled (blue) and atmosphere-only (red) simulations. Grey shading and horizontal lines extend from 5% to 95% confidence intervals of the observed/reanalysis and individual model internal variability feedback, respectively.

following, we aim to investigate whether extending the period used to estimate internal variability feedbacks can improve the potential for using observations to constrain forced climate feedbacks

3.2 The Relationship Between Internal Variability and Forced Climate Feedbacks During the ERA5 Reanalysis Period

Next, we utilize ERA5 reanalysis data as a surrogate for satellite observations. In a reanalysis, radiative fluxes are not directly constrained by observations but are derived from calculations based on the atmospheric state. While the distribution of temperature and water vapor in a reanalysis is relatively well-constrained, the representation of clouds is less constrained. Hence, to evaluate the extent to which ERA5 captures the patterns and variations observed in CERES data, we compare the detrended and deseasonalized TOA anomaly fluxes and internal variability feedbacks from ERA5 with those obtained from CERES over the overlapping time period 2001-2021 (Figures S3 and S4). In general, ERA5 captures the overall characteristics of the Earth's energy balance reasonably well, although discrepancies in the representation of longwave and shortwave radiation suggest potential limitations or uncertainties in accurately capturing the variability of these fluxes at TOA (Figure S3). Consequently, the discrepancies in the representation of radiative fluxes between ERA5 and CERES result in less pronounced longwave and shortwave internal variability feedbacks in ERA5 compared to that observed in CERES

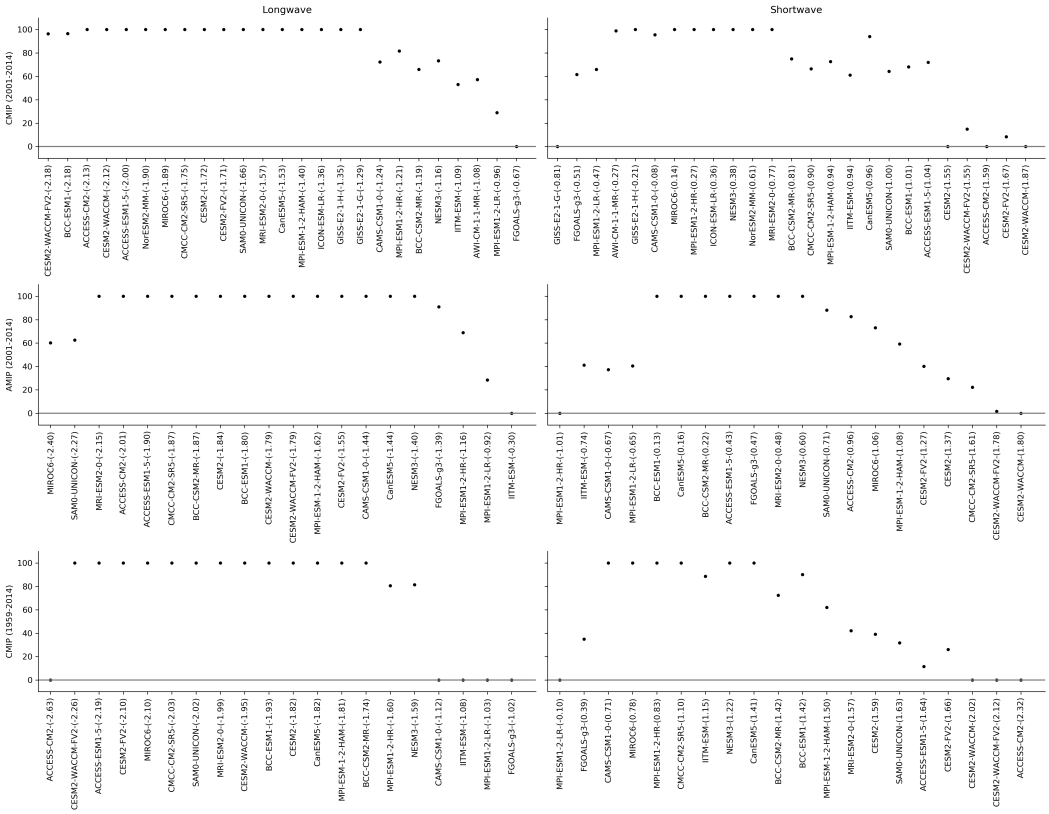

Figure 2. Probability of model uncertainty aligning with observed uncertainty, with the x-axis representing the arrangement of models in ascending order of feedback values (shown in parentheses).

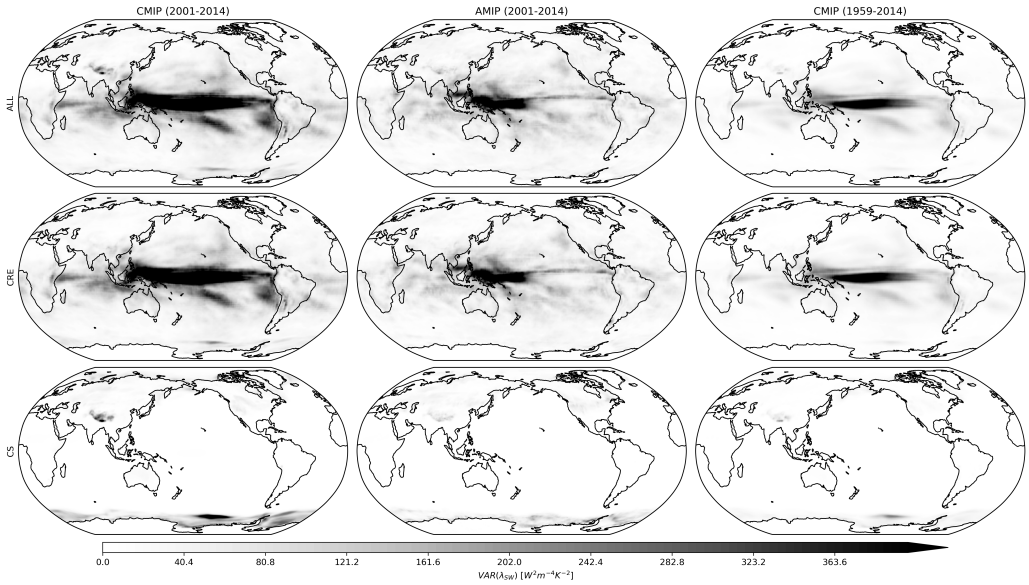

Figure 3. Maps of all-sky (top), cloud radiative effects (center), and clear-sky (bottom) shortwave internal variability variance for coupled (CMIP) and atmosphere-only (AMIP) models over the CERES (2001-2014) and ERA5 (1959-2014) periods.

data (Figure S4). Despite these disparities, the remarkable similarity between the reanalysis and the observed data indicates the potential value of the ERA5 for estimating internal variability feedbacks in situations where satellite observations are not available, for example for filling in short data gaps in satellite records.

We estimate reanalysis and simulated internal variability feedbacks focusing on their shared time period from 1959 to 2014. Note that here we use just historical coupled simulations since the time length of historical atmosphere-only simulations is shorter (1979-2014). To ensure the exclusion of volcanic forcings from the analysis, we specifically removed the years 1982-1983 and 1991-1992 from the time series since these years correspond to the eruptions of the El Chichon and Pinatubo volcanoes, which resulted in significant and rapid changes in TOA fluxes. Extending the analysis to this longer period enables a more comprehensive assessment of internal variability feedbacks, leading to a reduction in the uncertainty associated with both observed and simulated data (compare the confidence intervals over the short period in Figures 1a., 1b., 1c. to the long period in Figures 1d., 1e., 1f., as well as in Figure S4). In line with the findings from the analysis using the CERES period, the relationship between longwave and shortwave forced climate feedbacks and internal variability remains robust and significant when considering the ERA5 period (Figures 1d., 1e., and S1). This indicates that the relationship between longwave and shortwave internal variability and forced climate feedbacks is robust and consistent over an extended time span and increases the level of confidence that models exhibiting moderate negative longwave internal variability feedbacks, as well as moderate positive shortwave internal variability feedbacks, align more closely with observations (Figure 2). Nevertheless, the persistence of a large dispersion in the shortwave internal feedback (Figures S2 and 3) contributes to the absence of a significant relationship between net internal variability and net forced climate feedbacks (Figures 1f. and S1), which raises the question of whether such a relationship truly does not exist in CMIP6 models.

3.3 Emergence of the Relationship Between Net Internal Variability and Net Forced Climate Feedbacks

While the relationships between longwave and shortwave internal variability and forced climate feedbacks hold consistently for both short (CERES) and longer (ERA5) periods, a significant relationship has not been found for the net feedback component. To determine the existence of a relationship between net internal variability and net forced climate feedbacks in CMIP6 models, we extend our analysis to longer time periods beyond the limits of observational or reanalysis-based estimation of internal variability feedbacks.

To this end, we compute the correlation coefficient between net internal variability and net forced climate feedbacks across various time-window sizes in CMIP6 simulations, as well as the p-value through a hypothesis test assuming that the feedbacks are independent and uncorrelated. The calculation starts by using a 14-year historical simulation time window (2001-2014), and then extending the window by one year at a time until reaching the initial year of 1850 (1850-2014). The length of the historical simulations is 165 years; however, by excluding the years affected by volcanic eruptions (El Chichon, Pinatubo) as well as the years 1883 and 1884 (Krakatoa), the time series is reduced to 159 years.

The results reveal that significant relationships between net internal variability and net forced climate feedbacks do emerge (Figure 4). Such significant relationships stabilize when the net internal variability feedback is estimated using a time window of at least 60 years (1955-2014). However, due to the limited availability of observational data during this period, it is not possible to obtain an observational estimate of net internal variability feedback to constrain net forced climate feedbacks. Therefore, given the current

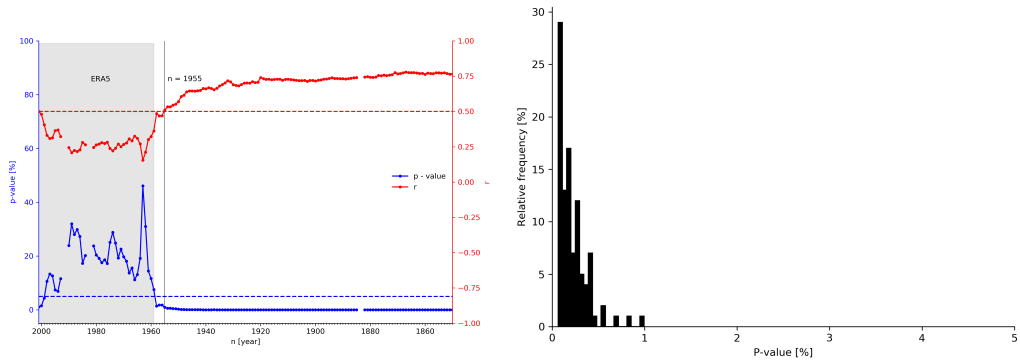

Figure 4. Left: Correlation (red) and p-value (blue) between net internal variability feedback estimated for the n - 2014 time window, and net forced climate feedback. Horizontal dashed lines indicates a correlation of 0.5 and a p-value of 5%, while the vertical line denotes the initial time window year when the relation approximately stabilizes. Grey area shows the period for which ERA5 reanalysis data is available. Right: P-value frequency distribution for uncorrelation tests between net internal variability and net forced climate feedbacks from CMIP6 coupled models over all 60-year windows between 1850 and 2014.

limitations of the available observational records, it is not currently possible to derive a constraint on net forced climate feedback using net internal variability feedbacks.

Combining the Earth Radiation Budget Experiment (ERBE) satellite record, which started in 1985, with the existing CERES data (Allan et al., 2014) would extend the available observational period to 37 years, thus about 24 years of continuous observational data would still need to be collected to reach a 60-year period. To assess the likelihood of a significant relationship between net internal variability and net forced climate feedbacks in CMIP6 coupled models over a 60-year window, other than 1955-2014, we calculate the frequency distribution of p-values between net internal variability and forced climate feedbacks for all potential 60-year continuous periods between 1850 and 2014 (Figure 4). The analysis reveals a high frequency of p-values below one percent, indicating a strong likelihood that, with an additional 24 years of satellite data, the use of observed net internal variability feedback as a constraint on net forced climate feedback would be highly feasible and reliable.

4 Conclusions

A study of the relationships between internal variability and forced climate feedbacks in models of the sixth generation of the Coupled Model Intercomparison Project is presented. Consistent with previous research (Uribe et al., 2022) we find evidence indicating that the strength of longwave and shortwave forced climate feedback relates to their internal variability feedback during the period of overlap between CERES data and historical simulations. Moreover, our results indicate that incorporating additional ensemble members in the estimation of internal variability feedbacks improves their robustness and representativeness, strengthening the relationship between internal variability and forced climate feedbacks.

Nevertheless, when combining the longwave and shortwave feedback components to estimate the net feedback, the relationship breaks down. A detailed examination highlighted that the presence of uncertainty in shortwave internal variability feedback, specifically related to cloud radiative effects in deep convective and subtropical stratocumu-

lus regions, as well as an inadequate compensation between shortwave and longwave internal variability feedbacks, significantly contributed to the diminished relationship between net internal variability and net forced climate feedbacks. On the other hand, the analysis of observed internal variability feedbacks based on satellite measurements indicates that models exhibiting strong and weak longwave feedbacks, as well as strong positive and strong negative shortwave feedbacks demonstrate a lower degree of agreement with observational data.

Further, we employed ERA5 reanalysis data to estimate internal variability feedbacks over an extended historical period spanning from 1959 to 2014. The analysis revealed a reduction in uncertainties associated with observed and simulated internal variability and confirmed the persistence of the relationship between longwave and shortwave feedbacks. These findings provide support for the hypothesis that models displaying moderate negative longwave feedbacks and moderate positive shortwave feedbacks are more consistent with observational data. Nevertheless, the relationship between net internal variability and net forced climate feedbacks remains weak.

Finally, using models only, we find that a statistically significant relationship between net internal and net forced climate feedbacks emerges when considering a period of at least 60 years. Given that the CERES record starts in 2000, our analysis suggests that it would be necessary to wait until approximately 2060 to accumulate 60 years of satellite observations. However, a possible solution to reduce this waiting time is to combine the CERES record with the Earth Radiation Budget Experiment (ERBE) satellite record (Allan et al., 2014), which could potentially shorten the time horizon to constraint to the mid-2040s.

5 Open Research

The CERES EBAF-TOA Ed4.1, data sets used for estimating observed TOA fluxes are available at the NASA Langley Research Center via `https://ceres.larc.nasa.gov/data/`. The Gridded temperature anomalies HadCRUT(5) data set used to estimate observed internal variability feedbacks can be obtained from the Met Office Hadley Centre observations datasets at `https://www.metoffice.gov.uk/hadobs/hadcrut5/`. Used CMIP6 models can be found in Table S1 and are available from ESGF at `https://esgf-node.llnl.gov`. ERA5 reanalysis data can be downloaded from the Copernicus Climate Change Service in `https://doi.org/10.24381/cds.f17050d7`.

Acknowledgments

The study was supported by the European Research Council project highECS (grant no. 770765), the Swedish Research Council (grant no. 2018-04274), the European Union's Horizon 2020 program projects CONSTRAIN (grant no. 820829) and NextGEMS (grant no. 101003470).

References

Allan, R. P., Liu, C., Loeb, N. G., Palmer, M. D., Roberts, M., Smith, D., & Vidale, P.-L. (2014). Changes in global net radiative imbalance 1985–2012. *Geophysical Research Letters*, *41*(15), 5588-5597. doi: https://doi.org/10.1002/2014GL060962

Brient, F., Schneider, T., Tan, Z., Bony, S., Qu, X., & Hall, A. (2016). Shallowness of tropical low clouds as a predictor of climate models'response to warming. *Climate Dynamics*, *47*(1), 433–449. doi: 10.1007/s00382-015-2846-0

Dessler, A. E. (2013). Observations of climate feedbacks over 2000–10 and comparisons to climate models. *Journal of Climate*, *26*(1), 333–342. doi: 10.1175/JCLI-D-11-00640.1

Dessler, A. E., & Forster, P. M. (2018). An estimate of equilibrium climate sensitivity from interannual variability. *Journal of Geophysical Research: Atmospheres*, *123*(16), 8634-8645. doi: https://doi.org/10.1029/2018JD028481

Dessler, A. E., Mauritsen, T., & Stevens, B. (2018). The influence of internal variability on earth's energy balance framework and implications for estimating climate sensitivity. *Atmospheric Chemistry and Physics*, *18*(7), 5147–5155. Retrieved from `https://acp.copernicus.org/articles/18/5147/2018/` doi: 10.5194/acp-18-5147-2018

Forster, P. T., K., S., W., A., J.-L., C., D., D., D.J., F., ... Zhang, H. (2021). The earth's energy budget, climate feedbacks, and climate sensitivity. [Book Section]. In V. Masson-Delmotte et al. (Eds.), *Climate change 2021: The physical science basis. contribution of working group i to the sixth assessment report of the intergovernmental panel on climate change* (chap. 7). Cambridge, United Kingdom and New York, NY, USA: Cambridge University Press. doi: 10.1017/9781009157896.009

Gregory, J. M., Ingram, W. J., Palmer, M. A., Jones, G. S., Stott, P. A., Thorpe, R. B., ... Williams, K. D. (2004). A new method for diagnosing radiative forcing and climate sensitivity. *Geophysical Research Letters*, *31*(3). doi: https://doi.org/10.1029/2003GL018747

Hargreaves, J. C., Annan, J. D., Yoshimori, M., & Abe-Ouchi, A. (2012). Can the last glacial maximum constrain climate sensitivity? *Geophysical Research Letters*, *39*(24). doi: https://doi.org/10.1029/2012GL053872

Hersbach, H., Bell, B., Berrisford, P., Hirahara, S., Horányi, A., Muñoz-Sabater, J., ... Thépaut, J.-N. (2020). The era5 global reanalysis. *Quarterly Journal of the Royal Meteorological Society*.

Jiménez-de-la Cuesta, D., & Mauritsen, T. (2019). Emergent constraints on earth's transient and equilibrium response to doubled co2 from post-1970s global warming. *Nature Geoscience*, *12*(11), 902–905. doi: 10.1038/s41561-019-0463-y

Loeb, N. G., Doelling, D. R., Wang, H., Su, W., Nguyen, C., Corbett, J. G., ... Kato, S. (2018). Clouds and the earth's radiant energy system (ceres) energy balanced and filled (ebaf) top-of-atmosphere (toa) edition-4.0 data product. *Journal of Climate*, *31*(2), 895 - 918. doi: 10.1175/JCLI-D-17-0208.1

Lutsko, N. J., Popp, M., Nazarian, R. H., & Albright, A. L. (2021). Emergent constraints on regional cloud feedbacks. *Geophysical Research Letters*, *48*(10), e2021GL092934. doi: https://doi.org/10.1029/2021GL092934

Mauritsen, T., & Stevens, B. (2015). Missing iris effect as a possible cause of muted hydrological change and high climate sensitivity in models. *Nature Geoscience*, *8*(5), 346–351. doi: 10.1038/ngeo2414

Morice, C. P., Kennedy, J. J., Rayner, N. A., Winn, J. P., Hogan, E., Killick, R. E., ... Simpson, I. R. (2021). An updated assessment of near-surface temperature change from 1850: The hadcrut5 data set. *Journal of Geophysical Research: Atmospheres*, *126*(3), e2019JD032361. doi: https://doi.org/10.1029/2019JD032361

NRC. (1979). *Carbon dioxide and climate: A scientific assessment*. Washington, DC: The National Academies Press. doi: 10.17226/12181

Renoult, M., Annan, J. D., Hargreaves, J. C., Sagoo, N., Flynn, C., Kapsch, M.-L., ... Mauritsen, T. (2020). A bayesian framework for emergent constraints: case studies of climate sensitivity with pmip. *Climate of the Past*, *16*(5), 1715–1735. Retrieved from `https://cp.copernicus.org/articles/16/1715/2020/` doi: 10.5194/cp-16-1715-2020

Sherwood, S. C., Webb, M. J., Annan, J. D., Armour, K. C., Forster, P. M., Hargreaves, J. C., ... Zelinka, M. D. (2020). An assessment of earth's climate sensitivity using multiple lines of evidence. *Reviews of Geophysics*, *58*(4), e2019RG000678. doi: https://doi.org/10.1029/2019RG000678

Trenberth, K. E., & Fasullo, J. T. (2010). Simulation of present-day and twenty-first-century energy budgets of the southern oceans. *Journal of Climate*, *23*(2), 440–454.

Uribe, A., Bender, F. A.-M., & Mauritsen, T. (2022). Observed and cmip6 modeled internal variability feedbacks and their relation to forced climate feedbacks. *Geophysical Research Letters*, *49*(24). doi: https://doi.org/10.1029/2022GL100075

Williamson, M. S., Thackeray, C. W., Cox, P. M., Hall, A., Huntingford, C., & Nijsse, F. J. M. M. (2021, May). Emergent constraints on climate sensitivities. *Rev. Mod. Phys.*, *93*, 025004. doi: 10.1103/RevModPhys.93.025004

Figure 1.

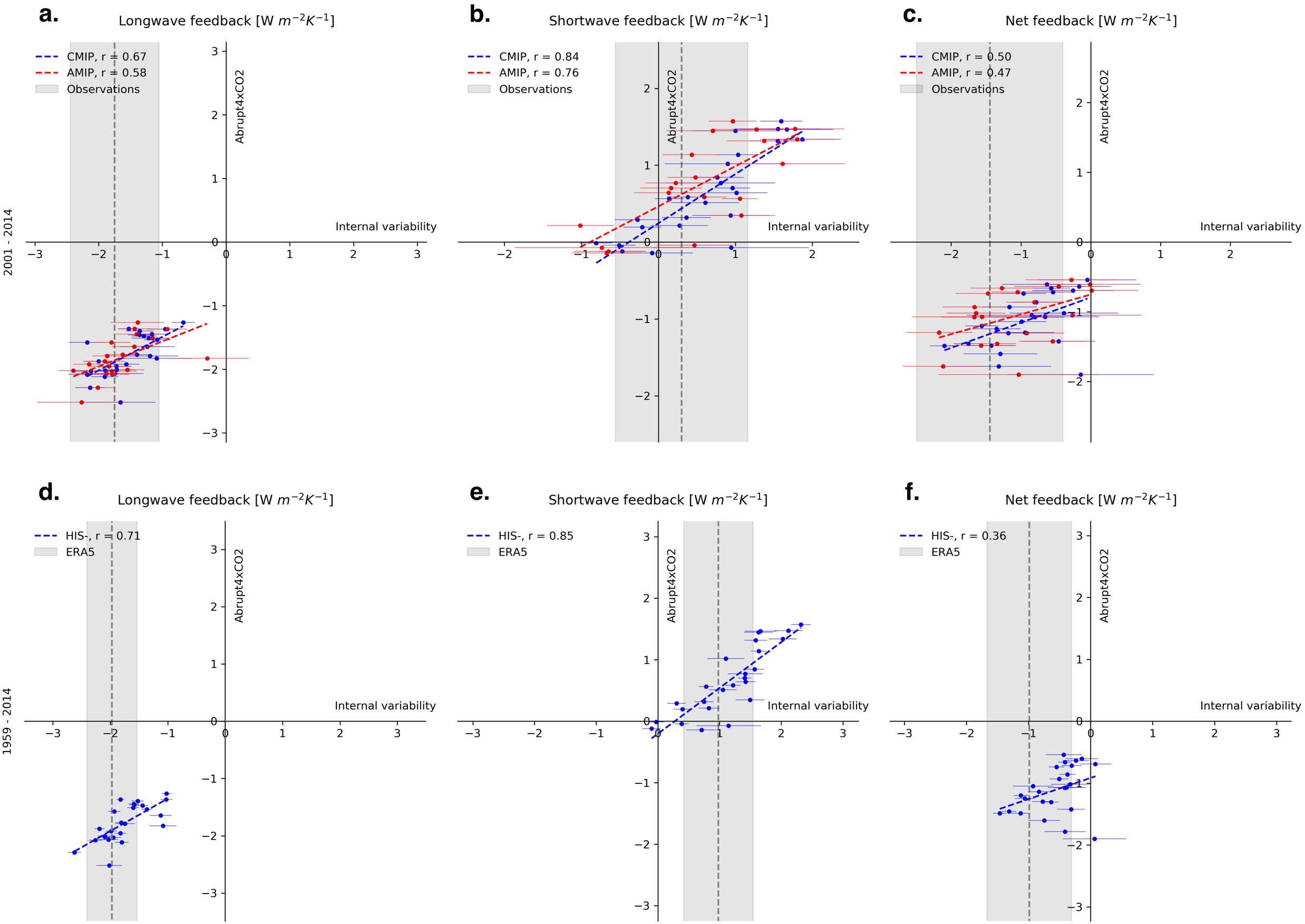
a.
Longwave feedback [W $m^{-2}K^{-1}$]
CMIP, r = 0.67
AMIP, r = 0.58
Observations
Abrupt4xCO2
Internal variability
2001 - 2014
b.
Shortwave feedback [W $m^{-2}K^{-1}$]
CMIP, r = 0.84
AMIP, r = 0.76
Observations
Abrupt4xCO2
Internal variability
c.
Net feedback [W $m^{-2}K^{-1}$]
CMIP, r = 0.50
AMIP, r = 0.47
Observations
Abrupt4xCO2
Internal variability
d.
Longwave feedback [W $m^{-2}K^{-1}$]
HIS-, r = 0.71
ERA5
Abrupt4xCO2
Internal variability
1959 - 2014
e.
Shortwave feedback [W $m^{-2}K^{-1}$]
HIS-, r = 0.85
ERA5
Abrupt4xCO2
Internal variability
f.
Net feedback [W $m^{-2}K^{-1}$]
HIS-, r = 0.36
ERA5
Abrupt4xCO2
Internal variability

Figure 2.

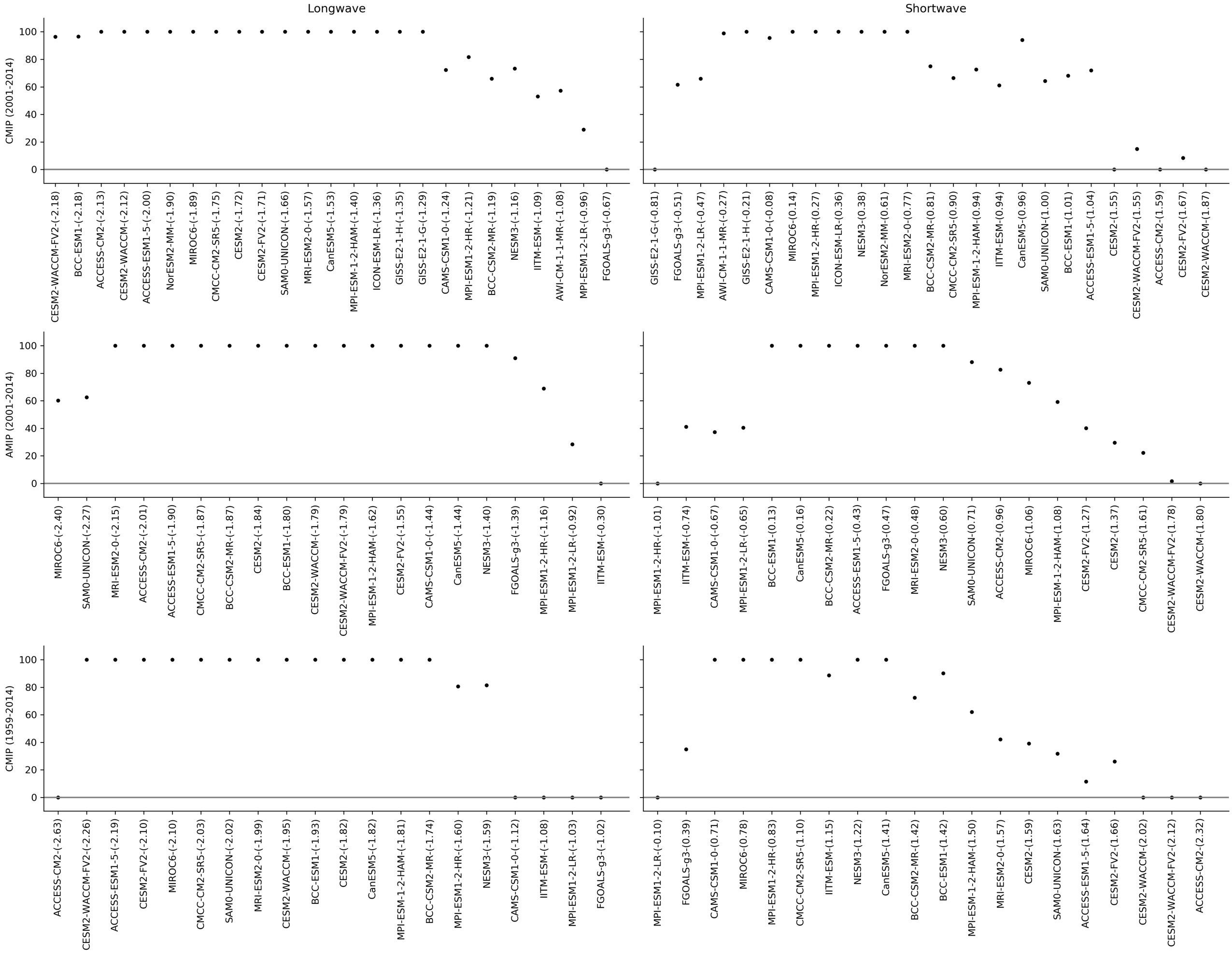
Longwave
Shortwave
CMIP (2001-2014)
AMIP (2001-2014)
CMIP (1959-2014)
0
20
40
60
80
100
CESM2-WACCM-FV2-(-2.18)
BCC-ESM1-(-2.18)
ACCESS-CM2-(-2.13)
CESM2-WACCM-(-2.12)
ACCESS-ESM1-5-(-2.00)
NorESM2-MM-(-1.90)
MIROC6-(-1.89)
CMCC-CM2-SR5-(-1.75)
CESM2-(-1.72)
CESM2-FV2-(-1.71)
SAM0-UNICON-(-1.66)
MRI-ESM2-0-(-1.57)
CanESM5-(-1.53)
MPI-ESM-1-2-HAM-(-1.40)
ICON-ESM-LR-(-1.36)
GISS-E2-1-H-(-1.35)
GISS-E2-1-G-(-1.29)
CAMS-CSM1-0-(-1.24)
MPI-ESM1-2-HR-(-1.21)
BCC-CSM2-MR-(-1.19)
NESM3-(-1.16)
IITM-ESM-(-1.09)
AWI-CM-1-1-MR-(-1.08)
MPI-ESM1-2-LR-(-0.96)
FGOALS-g3-(-0.67)
GISS-E2-1-G-(-0.81)
FGOALS-g3-(-0.51)
MPI-ESM1-2-LR-(-0.47)
AWI-CM-1-1-MR-(-0.27)
GISS-E2-1-H-(-0.21)
CAMS-CSM1-0-(-0.08)
MIROC6-(0.14)
MPI-ESM1-2-HR-(0.27)
ICON-ESM-LR-(0.36)
NESM3-(0.38)
NorESM2-MM-(0.61)
MRI-ESM2-0-(0.77)
BCC-CSM2-MR-(0.81)
CMCC-CM2-SR5-(0.90)
MPI-ESM-1-2-HAM-(0.94)
IITM-ESM-(0.94)
CanESM5-(0.96)
SAM0-UNICON-(1.00)
BCC-ESM1-(1.01)
ACCESS-ESM1-5-(1.04)
CESM2-(1.55)
CESM2-WACCM-FV2-(1.55)
ACCESS-CM2-(1.59)
CESM2-FV2-(1.67)
CESM2-WACCM-(1.87)
MIROC6-(-2.40)
SAM0-UNICON-(-2.27)
MRI-ESM2-0-(-2.15)
ACCESS-CM2-(-2.01)
ACCESS-ESM1-5-(-1.90)
CMCC-CM2-SR5-(-1.87)
BCC-CSM2-MR-(-1.87)
CESM2-(-1.84)
BCC-ESM1-(-1.80)
CESM2-WACCM-(-1.79)
CESM2-WACCM-FV2-(-1.79)
MPI-ESM-1-2-HAM-(-1.62)
CESM2-FV2-(-1.55)
CAMS-CSM1-0-(-1.44)
CanESM5-(-1.44)
NESM3-(-1.40)
FGOALS-g3-(-1.39)
MPI-ESM1-2-HR-(-1.16)
MPI-ESM1-2-LR-(-0.92)
IITM-ESM-(-0.30)
MPI-ESM1-2-HR-(-1.01)
IITM-ESM-(-0.74)
CAMS-CSM1-0-(-0.67)
MPI-ESM1-2-LR-(-0.65)
BCC-ESM1-(0.13)
CanESM5-(0.16)
BCC-CSM2-MR-(0.22)
ACCESS-ESM1-5-(0.43)
FGOALS-g3-(0.47)
MRI-ESM2-0-(0.48)
NESM3-(0.60)
SAM0-UNICON-(0.71)
ACCESS-CM2-(0.96)
MIROC6-(1.06)
MPI-ESM-1-2-HAM-(1.08)
CESM2-FV2-(1.27)
CESM2-(1.37)
CMCC-CM2-SR5-(1.61)
CESM2-WACCM-FV2-(1.78)
CESM2-WACCM-(1.80)
ACCESS-CM2-(-2.63)
CESM2-WACCM-FV2-(-2.26)
ACCESS-ESM1-5-(-2.19)
CESM2-FV2-(-2.10)
MIROC6-(-2.10)
CMCC-CM2-SR5-(-2.03)
SAM0-UNICON-(-2.02)
MRI-ESM2-0-(-1.99)
CESM2-WACCM-(-1.95)
BCC-ESM1-(-1.93)
CESM2-(-1.82)
CanESM5-(-1.82)
MPI-ESM-1-2-HAM-(-1.81)
BCC-CSM2-MR-(-1.74)
MPI-ESM1-2-HR-(-1.60)
NESM3-(-1.59)
CAMS-CSM1-0-(-1.12)
IITM-ESM-(-1.08)
MPI-ESM1-2-LR-(-1.03)
FGOALS-g3-(-1.02)
MPI-ESM1-2-LR-(-0.10)
FGOALS-g3-(0.39)
CAMS-CSM1-0-(0.71)
MIROC6-(0.78)
MPI-ESM1-2-HR-(0.83)
CMCC-CM2-SR5-(1.10)
IITM-ESM-(1.15)
NESM3-(1.22)
CanESM5-(1.41)
BCC-CSM2-MR-(1.42)
BCC-ESM1-(1.42)
MPI-ESM-1-2-HAM-(1.50)
MRI-ESM2-0-(1.57)
CESM2-(1.59)
SAM0-UNICON-(1.63)
ACCESS-ESM1-5-(1.64)
CESM2-FV2-(1.66)
CESM2-WACCM-(2.02)
CESM2-WACCM-FV2-(2.12)
ACCESS-CM2-(2.32)

Figure 3.

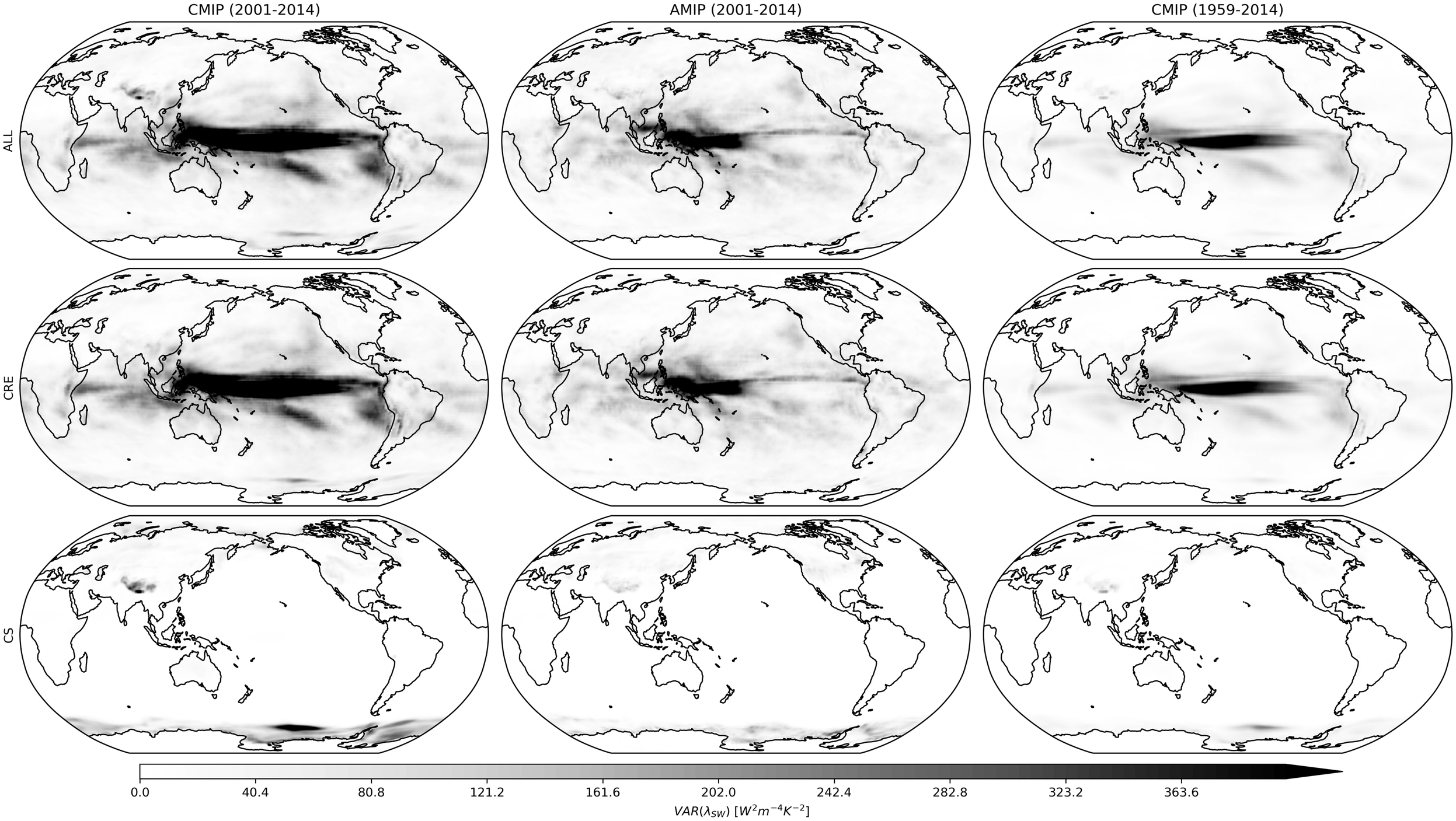
CMIP (2001-2014)
AMIP (2001-2014)
CMIP (1959-2014)
ALL
CRE
CS
0.0
40.4
80.8
121.2
161.6
202.0
242.4
282.8
323.2
363.6
$VAR(\lambda_{SW})$ $[W^2m^{-4}K^{-2}]$

Figure 4.

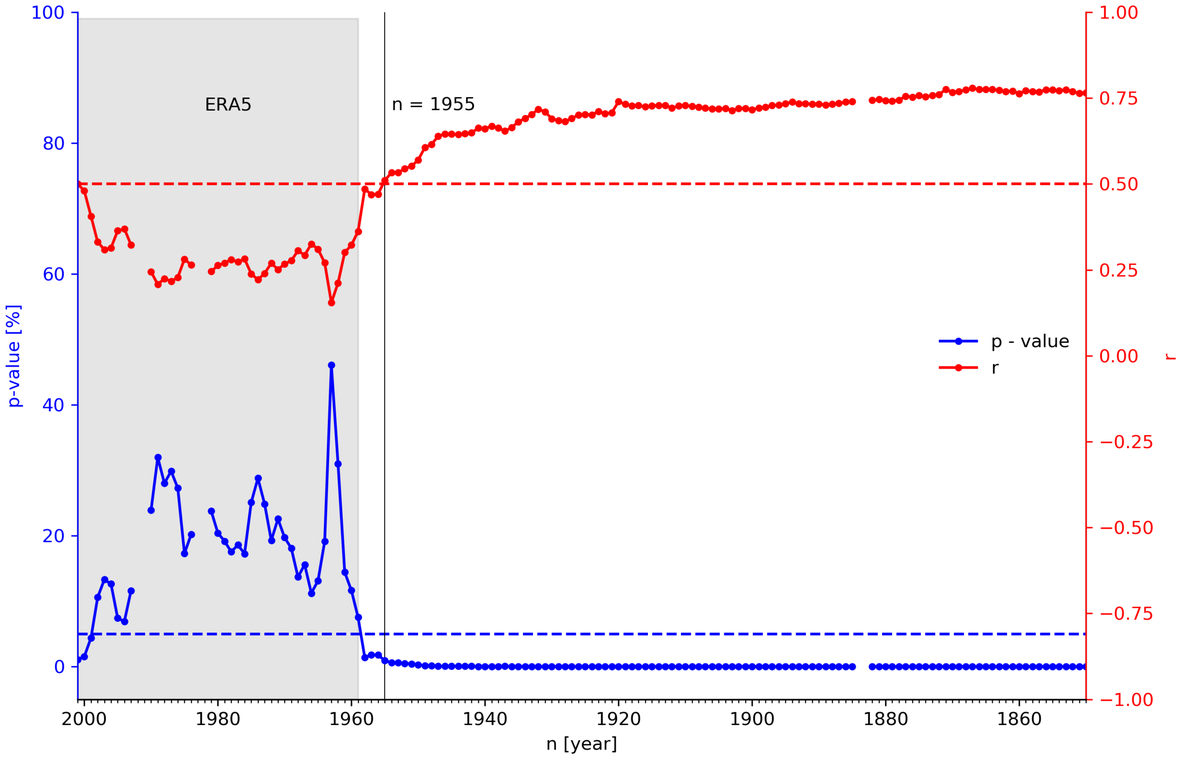
ERA5
n = 1955
p - value
r
p-value [%]
r
n [year]
100
80
60
40
20
0
1.00
0.75
0.50
0.25
0.00
−0.25
−0.50
−0.75
−1.00
2000
1980
1960
1940
1920
1900
1880
1860

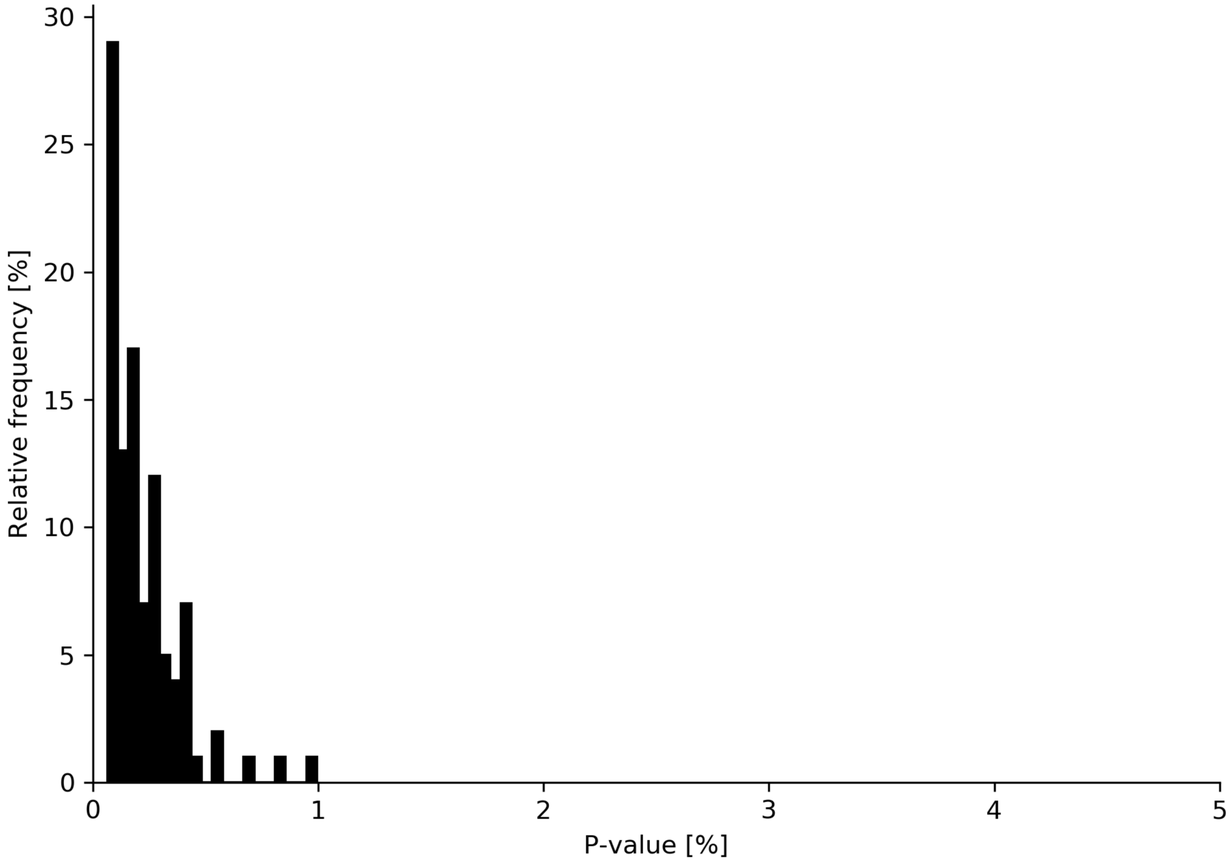
Relative frequency [%]
P-value [%]
30
25
20
15
10
5
0
0
1
2
3
4
5